

Ultrahigh-speed optical frequency domain imaging and application to laser ablation monitoring

W. Y. Oh,^{a)} S. H. Yun, B. J. Vakoc, G. J. Tearney, and B. E. Bouma
*Harvard Medical School and Wellman Center for Photomedicine, Massachusetts General Hospital,
 50 Blossom Street, BAR 704, Boston, Massachusetts 02114*

(Received 17 August 2005; accepted 12 January 2006; published online 10 March 2006)

We demonstrate a linear laser resonator incorporating a semiconductor optical amplifier and scanning filter for high repetition rate, broad wavelength, unidirectional scanning. The laser operates at up to 115 kHz repetition rates and demonstrates a tuning-speed-independent power of >30 mW. We apply this laser to enable ultrahigh-speed optical frequency domain imaging of the dynamics of laser ablation of biological tissue. The imaging system acquires single longitudinal scans (A-lines) in $8.7 \mu\text{s}$ and complete cross-sectional images comprising 575 A-lines at a rate of 200 frames per second. © 2006 American Institute of Physics. [DOI: 10.1063/1.2179125]

Optical coherence tomography (OCT) allows cross-sectional imaging of optically turbid samples at spatial resolutions on the order of several to tens of microns. In the biomedical field, OCT has been used to image various tissues and has been shown to be capable of screening for disease. Traditional OCT system imaging speeds were limited to four to eight frames per second, suitable for directed, small-area imaging but unable to allow OCT to either provide comprehensive microscopic screening¹⁻³ or image dynamic events, such as laser ablation of tissue.⁴⁻⁷ The recent application of Fourier-domain techniques to OCT has led to an improvement in sensitivity of several orders of magnitude, a critical step toward ultrahigh-speed OCT imaging.⁸⁻¹⁰ Optical frequency domain imaging (OFDI)^{8,11} is one of the Fourier approaches and is conceptually a two- or three-dimensional extension of optical frequency domain reflectometry (OFDR),¹²⁻¹⁴ which uses a wavelength-swept light source and interferometer for heterodyning. Realizing the potential imaging speed improvement of OFDI, however, requires the development of new high-repetition rate wavelength-swept lasers. In this letter, we present a novel external cavity semiconductor laser that provides wavelength-swept light from 1280 nm to 1360 nm at continuously tunable repetition rates up to 115 kHz, and demonstrates an OFDI system, based on this source, that can continuously acquire cross-sectional images at a rate of 200 images (575 A-lines per image) per second. To demonstrate the capability of this ultrahigh-speed system, the measured dynamics of tissue ablation, too fast to be imaged by traditional OCT systems, are presented.

In OFDI, the ranging depth is inversely proportional to the instantaneous linewidth of the source, the axial resolution is inversely proportional to the wavelength range over which the source is swept, and the detection sensitivity is proportional to the laser power. Relevant laser source specifications for OFDI include an instantaneous linewidth less than 0.1 nm, a tuning range greater than 10% of the central wavelength, and an average power greater than 20 mW in a single polarization state. Based on theoretical analyses,^{8,11} a source achieving these specifications would provide sufficient detection sensitivity for biomedical imaging even at an axial ranging (A-line) rate greater than 100 kHz. We have previ-

ously demonstrated a rapidly tuning optical filter¹⁵ and semiconductor ring resonator¹⁶ that provided a scanning rate of 115 kHz. One complicating characteristic of this laser, however, is the power and linewidth dependence upon tuning speed. At fast tuning speeds, the filter offset per round trip of the resonator becomes significant compared with the filter bandwidth, resulting in a decrease in the output power and an increase in the instantaneous linewidth of the laser.¹⁶ One approach to reduce this effect would be to match the filter tuning period to an integer fraction of the laser round-trip time.¹⁷ In this case, the light circulating in the resonator has a continuously varying wavelength, such that at the location of the filter the wavelength varies in synchrony with the filter allowing the buildup of a stable resonator mode. For a filter repetition rate of 100 kHz, however, the required resonator optical path length would be 3 km. Although this length is achievable for an optical fiber resonator, the long length of fiber may give rise to nonlinearities and thermal instabilities. An alternative approach, demonstrated in this letter, is to reduce the resonator round trip time so that light transmitted through the filter returns to the filter before the filter pass-band has significantly offset. As with the synchronous resonator approach, this provides a long photon intracavity lifetime and promotes laser linewidth narrowing.

To investigate the performance of a wavelength-swept laser having a reduced resonator length, we developed a semiconductor optical amplifier (SOA) having one normal incidence waveguide facet and one angled facet. The normal incidence facet was used as the output coupler of a linear resonator (transmission $\sim 70\%$). Light emitted from this facet was directly coupled to single-mode fiber. Light from the angled facet was collimated and coupled to an optical filter based on a diffraction grating, telescope, and rotating polygon scanner. Figure 1 shows the schematic of the laser. The optical path length of the linear resonator was 1.08 m, corresponding to a round trip time of 3.6 ns. When operating the filter over a sweep range of 80 nm and with a sweep repetition rate of 115 kHz, the offset of the filter center wavelength per roundtrip was 0.03 nm. For our filter pass-band width of 0.15 nm, we estimate that the loss arising from this offset was 13%. This loss was easily tolerated by the SOA, which had a single-pass gain of 25 dB.

^{a)}Electronic mail: woh1@partners.org

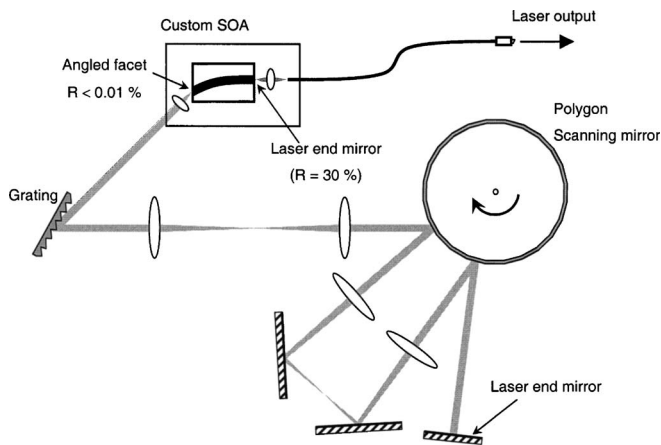


FIG. 1. A schematic of the linear cavity wavelength-swept laser. SOA: Semiconductor optical amplifier.

An additional advantage of the reduced resonator length is that it supports a broader detection bandwidth in OFDI. Resonator longitudinal mode beating gives rise to intensity noise at the characteristic frequency of the mode spacing and its harmonics. It is highly desirable that these frequencies do not overlap with the broad signal spectrum of high-speed OFDI. Since the longitudinal mode spacing is inversely proportional to the cavity length, the 1.08 m cavity length of the linear resonator avoids intensity noise corruption of the OFDI signal over the frequency range up to 280 MHz.

Figure 2(a) shows the peak power of the laser over an 80 nm edge to edge wavelength tuning range for different sweep speeds. The peak output power was measured to be constant while the tuning repetition rate was increased from 45 kHz to 115 kHz. We also characterized the instantaneous linewidth of the laser for various tuning repetition rates by measuring the coherence length of the laser output using a variable-delay Michelson interferometer [Fig. 2(b)]. A slight broadening of the instantaneous linewidth, from 0.15 nm to 0.16 nm, was observed as the tuning speed was increased from 45 kHz to 115 kHz. By comparison, a longer (5.2 m), fiber ring resonator using the same optical filter,¹⁶ exhibited a significant dependence of linewidth upon scanning speed. The linewidth of that laser was 0.23 nm at a repetition rate of 115 kHz.

Figure 3 depicts a schematic of the OFDI system employing the linear-cavity wavelength-swept laser for imaging of laser ablation dynamics. The system is comprised of a single-mode-fiber interferometer with dual-balanced detection¹¹ and acousto-optic frequency shifters to remove depth degeneracy.¹⁸ A transistor-transistor logic (TTL) pulse

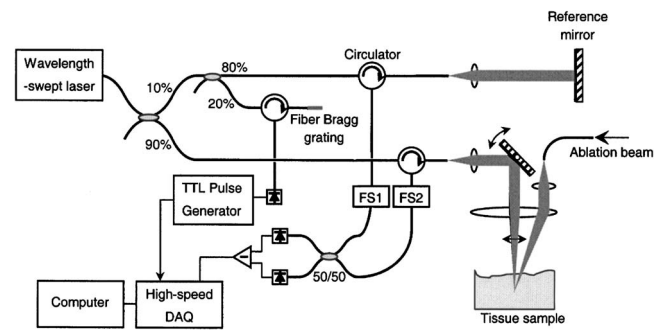


FIG. 3. A schematic of the OFDI system for monitoring of laser ablation. FS: Frequency shifter.

train generated from a fiber Bragg grating was used to provide synchronization pulses for signal sampling. A high-speed data acquisition (DAQ) board (Gage, CompuScope 14200) digitized the dual-balanced receiver output with a 100 MHz sampling frequency. The measured ranging depth defined at the 6 dB signal-to-noise ratio penalty¹⁸ is depicted in Fig 2(b). We note that the ranging depth of >4.8 mm is significantly improved over that of standard time-domain OCT systems even though the scanning speed has been increased more than 50 fold. The sensitivity was approximately 105 dB at zero delay, approximately 10 dB above the shot noise limit due to thermal and intensity noise contributions.

To demonstrate the potential of this system for monitoring dynamic processes, the system was configured to permit simultaneous imaging and laser ablation of biological samples. Laser ablation is commonly used in clinical medicine to dissect and remove tissue with the central goal to effectively treat targeted tissue while minimizing damage to adjacent tissue. To help understand and thereby improve the efficacy of ablation in medicine, rigorous models of the dynamics of tissue ablation have been developed.⁴ These models describe dynamic processes, such as tissue vaporization and vapor bubble formation and collapse. We sought to investigate the potential of ultrahigh-speed OFDI for monitoring ablation dynamics as a potential means to: (1) Test and refine existing models,⁴ and (2) provide feedback to improve the selectivity of treatment. A gated continuous-wave laser diode, centered at 1450 nm, was focused at the center of the OFDI transverse scan line (depicted in Fig. 3). During imaging, the 1450 nm laser power and exposure duration could be adjusted by controlling the diode current and gate duration. Images of freshly excised porcine esophagus, comprising 575 A-lines, were acquired at a rate of 200 frames per second for a range of ablation power and exposure duration. Continuous acquisition at this rate could be sustained for over 500 sequential images spanning 2.8 s. A movie of the laser ablation is available via EPAPs.¹⁹ A subset of sequential images acquired during ablation with 600 mW is shown in Fig. 4. The first image of the series was acquired 90 ms after the onset of 1450 nm laser exposure. Within the first 20 ms (four frames), a vapor bubble is observed that subsequently bursts prior to reforming in Frame No. 8. We believe that the ability to monitor temporal dynamics, such as these, during the ablation process may provide a new method for reducing collateral damage to adjacent tissue while ensuring comprehensive treatment of targeted tissues.

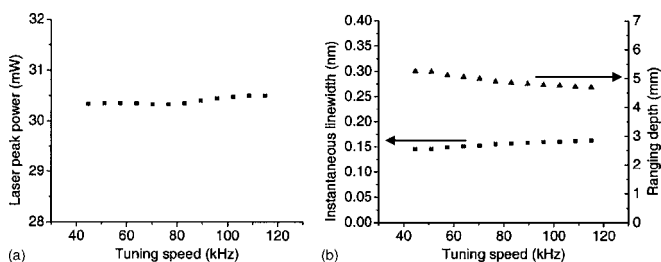


FIG. 2. (a) Peak power of the laser output measured for different wavelength tuning speed. (b) Instantaneous linewidth of the laser output (square), and corresponding ranging depth in OFDI (triangle) for different wavelength tuning speed.

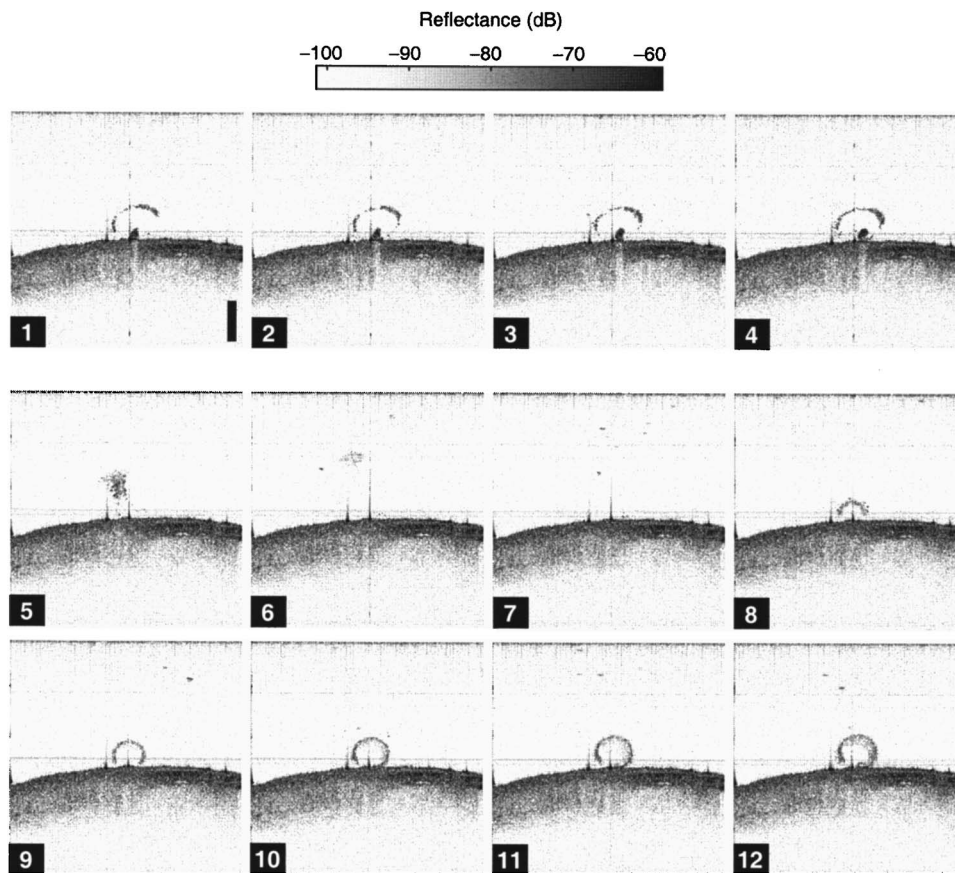


FIG. 4. A series of OFDI images acquired every 5 ms. Each images comprised of 320 axial \times 575 transverse pixels plotted in logarithmic inverse grayscale. The scale bar represents 1.0 mm.

In summary, we have demonstrated a novel linear-external-cavity wavelength-swept semiconductor laser that provided repetition rates up to 115 kHz. The short linear resonator was seen to significantly reduce the dependence of power and linewidth on tuning speed. We also demonstrated an ultrahigh-speed OFDI system, based on this laser, which was capable of imaging at an acquisition rate of 200 frames per second for images consisting of 575 A-lines over a depth range of 4.8 mm. We believe this unique ultrahigh-speed imaging system will open many new biomedical imaging applications and have demonstrated its ability to monitor dynamical processes during laser ablation.

This research was supported in part by the National Institutes of Health, Contract Nos. R01 HL70039, R33 CA110130, and R01 HL076398, and by the Terumo Corporation.

¹B. E. Bouma, G. J. Tearney, C. C. Compton, and N. S. Nishioka, *Gastrointest Endosc* **51**, 467 (2000).

²I. K. Jang, B. E. Bouma, D. H. Kang, S. J. Park, S. W. Park, K. B. Seung, K. B. Choi, M. Shishkov, K. Schlendorf, E. Pomerantsev, S. L. Houser, H. T. Aretz, and G. J. Tearney, *J. Am. Coll. Cardiol.* **39**, 604 (2002).

³G. J. Tearney, H. Yabushita, S. L. Houser, H. T. Aretz, I. K. Jang, K. Schlendorf, C. R. Kauffman, M. Shishkov, E. F. Halpern, and B. E. Bouma, *Circulation* **106**, 113 (2003).

⁴A. Vogel and V. Venugopalan, *Chem. Rev. (Washington, D.C.)* **103**, 577 (2003).

⁵N. A. Patel, X. Li, D. L. Stamper, J. G. Fujimoto, and M. E. Brezinski, *Int.*

J. Card. Imaging **19**, 171 (2003).

⁶S. A. Boppart, J. Herrmann, C. Pitris, D. L. Stamper, M. E. Brezinski, and J. G. Fujimoto, *J. Surg. Res.* **82**, 275 (1999).

⁷B. D. Goldberg, N. Ifimia, G. J. Tearney, and B. E. Bouma, in *Proceedings of the OSA Biomedical Optics Topical Meetings* (Optical Society of America, Miami Beach, FL, 2004).

⁸M. A. Choma, M. V. Sarunic, C. Yang, and J. A. Izatt, *Opt. Express* **11**, 2183 (2003).

⁹J. F. de Boer, B. Cense, B. H. Park, M. C. Pierce, G. J. Tearney, and B. E. Bouma, *Opt. Lett.* **28**, 2067 (2003).

¹⁰R. Leitgeb, C. K. Hitzenberger, and A. F. Fercher, *Opt. Express* **11**, 889 (2003).

¹¹S. H. Yun, G. J. Tearney, J. F. de Boer, N. Ifimia, and B. E. Bouma, *Opt. Express* **11**, 2953 (2003).

¹²W. Eickhoff and R. Ulrich, *Appl. Phys. Lett.* **39**, 693 (1981).

¹³B. Golubovic, B. E. Bouma, G. J. Tearney, and J. G. Fujimoto, *Opt. Lett.* **22**, 1704 (1997).

¹⁴A. J. Fercher, C. K. Hitzenberger, G. Kamp, and S. Y. Elzaiat, *Opt. Commun.* **117**, 43 (1995).

¹⁵S. H. Yun, C. Boudoux, G. J. Tearney, and B. E. Bouma, *Opt. Lett.* **28**, 1981 (2003).

¹⁶W. Y. Oh, S. H. Yun, G. J. Tearney, and B. E. Bouma, *Opt. Lett.* **30**, 3159 (2005).

¹⁷J. M. Telle and C. L. Tang, *Appl. Phys. Lett.* **26**, 572 (1975).

¹⁸S. H. Yun, G. J. Tearney, J. F. de Boer, and B. E. Bouma, *Opt. Express* **12**, 4822 (2004).

¹⁹See EPAPS Document No. E-APPLAB-88-007609 for avi movie of the ultrahigh-speed OFDI imaging of the laser ablation. A direct link to this document may be found in the online article's HTML reference section. The document may also be reached via the EPAPS home page (<http://www.aip.org/pubserus/epaps.html>) or from <ftp.aip.org> in the directory /epaps/. See the EPAPS home page for more information.